Cellular Physiology and Biochemistry

Cell Physiol Biochem 2020;54:384-400
DOI: 10.33594/000000226
Published online: 23 April 2020
Accepted: 22 March 2020

Original Paper

Fat Quality Matters: Distinct Proteomic Signatures Between Lean and Obese Cardiac Visceral Adipose Tissue Underlie its Differential Myocardial Impact

Glória Conceição[a] Júlia Matos[b] Daniela Miranda-Silva[a] Nádia Gonçalves[a] Cláudia Sousa-Mendes[a] Alexandre Gonçalves[a] Rita Ferreira[c] Adelino F. Leite-Moreira[a,d] Rui Vitorino[a,b] Inês Falcão-Pires[a]

[a]Cardiovascular Research and Development Center, Faculty of Medicine of the University of Porto, Porto, Portugal, [b]Department of Medical Sciences, iBiMED, Institute of Biomedicine, University of Aveiro, Aveiro, Portugal, [c]QOPNA, Department of Chemistry, University of Aveiro, Aveiro, Portugal, [d]Department of Cardiothoracic Surgery, São João Hospital Centre, Porto, Portugal

Key Words
Cardiac visceral adipose tissue • Heart failure with preserved ejection fraction • Proteome • Obesity • ZSF1 rats

Abstract
Background/Aims: Heart failure with preserved ejection fraction (HFpEF) is recognised as an important cause of cardiovascular mortality and morbidity, accounting for approximately 50% of heart failure cases. Metabolic-related complications, such as obesity, have been associated with the pathophysiology of this complex syndrome. The anatomic proximity between cardiac visceral adipose tissue (CVAT) and the myocardium has been drawing attention due to its potential pathogenic role in cardiac diseases. Thus, we aimed to characterise the phenotypic and proteomic differences between CVAT from ZSF1 lean (control) and ZSF1 obese (HFpEF) rats as well as to evaluate the myocardial impact of conditioned media derived from CVAT of these 2 groups. ***Methods:*** CVAT of 20-weeks-old lean and obese ZSF1 rats was collected for: 1) 24h DMEM incubation to obtain conditioned media, 2) separation of proteins to mass spectrometry identification, 3) adipokines' expression, 4) adipocytes cross-sectional area assessment. Organotypic cultures were prepared from 7 days-old Wistar Han cardiac explants and incubated for 24h with the conditioned media. After incubation, cross-section area of cardiomyocytes and fibrosis were evaluated. Cardiomyocytes were isolated from Wistar Han and incubated with conditioned media for viability studies. ***Results:*** CVAT from lean rats presented a higher expression of uncoupling protein-1 (UCP-1) protein, associated with a multilocular appearance and an increased expression of brown adipose tissue markers.

Inês Falcão-Pires, PhD
Department of Surgery and Physiology, Faculty of Medicine, Universidade do Porto
Alameda Prof. Hernâni Monteiro, 4200-319 Porto (Portugal)
Tel. +351 220 426 805, Fax +351 225 513 646, E-Mail ipires@med.up.pt

Contrarily, CVAT from obese rats revealed a white adipose tissue-like phenotype accompanied by hypertrophy of adipocytes. The analysis of the CVAT proteome reinforced the phenotypic differences between lean and obese CVAT, showing enrichment of proteins involved in triglyceride metabolic processes in obese CVAT. In contrast, mitochondrial proteins were prominent in lean CVAT, further suggesting a brown adipose tissue-like phenotype. The twenty-four hours-long incubation of myocardial organo-cultures with conditioned media obtained from CVAT obese (CM-obese) rats significantly reduced cell viability, induced cardiomyocytes hypertrophy and fibrosis, in stark contrast with the incubation with the conditioned media from lean rats CVAT (CM-lean). Furthermore, the deleterious effect imposed by CM-obese was associated with a pro-inflammatory profile, characterised by an increased expression of several pro-inflammatory adipokines. ***Conclusion:*** Obesity promotes alterations in CVAT proteome signature, structure, composition and secretome, translating into dramatic myocardial consequences.

Introduction

Heart failure with preserved ejection fraction (HFpEF) is a major and growing clinical epidemiological problem worldwide, whose prevalence has strikingly grown due to rising incidence of risk factors in the ageing population [1]. These patients exhibit a large number of comorbidities, including obesity, diabetes mellitus and hypertension [1]. Therefore, HFpEF is regarded as a cardiac multifactorial disease, largely influenced by systemic comorbidities [2].

It is well established that obesity confers an increased risk of developing cardiovascular diseases (CVD) [3]. The prevalence of obesity and associated risk factors has escalated to alarming levels and has become a worldwide epidemic [4]. This has motivated extensive research in the biology of adipose tissue and in its pathophysiological role in obesity-related complications. The classic view of adipose tissue as an inert lipid storage has evolved and it is now perceived as a metabolically dynamic endocrine organ capable of synthesising biologically active molecules that regulate metabolic homeostasis, as well as a diversity of biological functions [5].

Numerous fat depots, which may serve specialized functions, relate to their neighbouring tissues. Cardiac visceral adipose tissue (CVAT) is the visceral adipose tissue located around the heart [6, 7]. CVAT is principally composed of epicardial, pericardial and pericoronary adipose tissue, providing metabolic-mechanical support to the heart and to the blood vessels under physiologic conditions [7, 8]. Several studies, however, have recognised epicardial fat as an independent determinant of the development and progression of coronary artery disease [9, 10]. Thus, CVAT most likely affects myocardial structure and function [11]. So, it is mandatory to understand the specific influence of CVAT in the pathological mechanisms triggering myocardial disease in obesity-related complications.

The obese ZSF1 rat represents a good model of metabolic syndrome since it displays hypertension and obesity-related complications, such as type 2 diabetes mellitus (T2DM), insulin resistance, hyperinsulinaemia, hypertriglyceridaemia and hypercholesterolaemia [2]. We have previously described that all these obesity-related complications trigger HFpEF in 20 weeks-old obese ZSF1 rats, which also showed effort intolerance and significant diastolic dysfunction with preserved ejection fraction [12-15]. Therefore, the ZSF1 obese rat represents a robust model of metabolic dysfunction-induced HFpEF [2].

In this context, the purpose of the present work was to characterise changes in CVAT structure, composition and secretory profile under conditions of obesity-induced HFpEF and to assess its potential impact in cardiac structure.

Materials and Methods

Animals

All the procedures in this work followed the recommendations of the Guide for the Care and Use of Laboratory Animals, published by the US National Institutes of Health (NIH Publication No. 85-23, Revised 2011) and were certified by the Portuguese Veterinary Governmental Authorities and by the ethical committee of the institution. Only trained researchers, certified with a Laboratory Animal Science course according to the Federation of European Laboratory Animal Science Associations, handled animals and performed animal procedures.

Neonatal and adult Wistar Han rats (n=6) were sacrificed for organo-culture experiments and isolation of cardiomyocytes, respectively. Additionally, nine-weeks-old lean ZSF1 (Lean, n=10) and obese ZSF1 (Obese, n=10) rats (Charles River, Barcelona, Spain) were housed in groups of two animals/cage in individually ventilated chambers, maintained on a 12h light-dark cycle, with free access to food (LabDiet® 5008, International Product Supplies Ltd.) and water. One week before the end of the protocol, animals underwent blood collection, metabolic and echocardiographic evaluations as described in [12, 16]. At 20 weeks of age, anesthetised animals (8% for induction and 2.5-3% for maintenance) underwent a haemodynamic evaluation and were sacrificed by exsanguination with collection of blood and CVAT (Fig. 1) samples for histologic, molecular and cellular studies.

Preparation of conditioned media

Immediately after collection, CVAT was washed with phosphate buffered saline (PBS), macerated and incubated in 100 mg/mL Dulbecco's Modified Eagle Medium (DMEM, Gibco) supplemented with 1% penicillin/streptomycin (Pen/Strep, Gibco), at 37˚C in a humidified incubator (BINDER, USA) with 5% CO_2. After 24h in culture, the conditioned media (CM) from Lean (CM-lean) and Obese (CM-obese) ZSF1 rats were collected and stored at -80˚C and their subsequent use in cardiac organo-cultures.

Myocardial organo-cultures of neonatal rats

To study the effect of adipose tissue-conditioned media, we performed an organo-culture model of the neonatal rat heart [17]. Cardiac organo-cultures were obtained from neonatal (7 days of age) Wistar Han rats. Ventricles of the neonatal rats were excised, placed on heart matrix and cut in four sagittal slices with a thickness of 1 mm (Harvard Apparatus, Stainless Steel Coronal Brain, USA). For a liquid-air interface, slices were posed in semi-porous tissue culture inserts (Millicell, Cell Culture Inserts, Germany) and placed in a six-well culture plate with 1 mL of culture solution DMEM containing 10% FBS and 1% Pen/Strep. Heart slices were cultured at 37˚C in humidified air with 5% CO_2. In a different set of experiments, heart slices were treated, in triplicate, with CVAT-conditioned media and culture media alone for 24 hours. At the end of the experiment, heart slices were washed with PBS and fixed with 4% formaldehyde.

Isolation of adult rat cardiomyocytes

Ventricular cardiomyocytes were isolated by enzymatic dissociation as described previously [18-20]. Cardiomyocytes were plated on laminin-coated plates using M199 media and incubated at 37°C in humidified air with 5% CO_2.

Evaluation of cardiomyocyte viability

In a different set of tests, rat cardiomyocytes were seeded in a 96-well plate, in triplicate, at a density of 8-10 x 10^3 cells per well in 200 µL of M199 (control) or CVAT-conditioned media (CM-lean and CM-obese). Resazurin (0.0125%) was added to the medium (10% of cell culture volume) and incubated at 37°C. After 3 hours of incubation, absorbance was measured using a spectrophotometer set at 570 nm (Tecan).

Quantitative histomorphologic analysis

Histomorphometric analysis of heart slices was performed on Sirius red- and haematoxylin-and-eosin-stained 3 µm-thick-sections of tissue fixated in 4% formaldehyde. Section images were acquired with a microscope (x400, Olympus XC30 Digital colour Camera) and analysed using imaging software (Cell^B, Olympus) and image analysis software (ImageJ) to determine cardiomyocyte cross-sectional area (50 cardiomyocytes per group) and myocardial fibrosis, respectively. Fibrosis was calculated as the sum of all

connective tissue areas divided by the sum of connective tissue and muscle areas averaged over 4 to 6 representative fields of the section, as previously described [21].

Histomorphometric analysis of CVAT was performed in haematoxylin-and-eosin-stained 3-μm-thick-sections after 4% formaldehyde fixation. Stained sections of slides were digitally photographed (Olympus XC30 Digital colour Camera) and adipocytes cross-sectional area measured using imaging software (Cell B, Olympus). The average adipocyte cross-sectional area was determined after measuring all adipocytes in 10 fields for each animal (n = 7/group).

Protein extraction procedure

CVAT samples were washed three times with cold PBS to remove excess blood contamination. Then, adipose tissue (with approximately 0.1 – 0.2 g wet weight) were homogenized in 125 mM Tris-HCl, 2% sodium dodecyl sulphate (SDS), 50 mM dithiothreitol (DTT), 8 M urea, 2 M thiourea, 2% 3-[(3-cholamidopropyl) dimethylammonio] propane sulfonate (CHAPS), 2% ampholytes (pH 3-10), 1% NP-40, 50 mM DTT and 10 μL PMSF using a Potter-Elvehjem with a Teflon pestle. The lysate was centrifuged at 14, 000*g* for 30 min at 4°C and the supernatant was carefully collected. Protein concentration was estimated using RC-DC Protein assay (Bio-Rad, Hercules, CA, USA) (n = 3/group).

Protein identification and quantification

CVAT sample (50 μg of protein) was separated using 15% SDS-PAGE prepared, as previously described [22]. Complete lanes were cut out of the gel and sliced into 16 sections. Proteins in each section were digested in-gel with trypsin. The resulting peptide mixture was then extracted from the gel fractions and dried using vacuum centrifugation.

The dried extracted peptides were dissolved in 10 μL of mobile phase A (0.1% trifluoroacetic acid, 5% acetonitrile, 95% water). All peptide mixtures were analysed in two separate runs. The tryptic digests were separated using an Ultimate 3000 (Dionex, Sunnyvale, CA) onto a 150 mm × 75 μm Pepmap100 capillary analytical C18 column with 3 μm particle size (Dionex, LC Packings) at a flow rate of 300 nL/min. The gradient started at 10 min and ramped to 50% Buffer B (85% acetonitrile, 0.04% trifluoracetic acid) over 45 min. The peptides eluting from the column were mixed with a continuous flow of matrix solution (270 nL/min, 2 mg/mL α-CHCA in 70% ACN/0.3% TFA and internal standard Glu-Fib at 15 fmol) in a fraction microcollector (Probot, Dionex/LC Packings) and directly deposited onto the LC-MALDI plates at 20s intervals for each spot.

Samples were analysed using a 4800 MALDI-TOF/TOF Analyzer (AbSCIEX). A S/N threshold of 50 was used to select peaks for MS/MS analyses. The spectra were processed using the TS2Mascot (v1.0, Matrix Science Ltd) and submitted to Mascot software (v.2.1.0.4, Matrix Science Ltd) for peptide/protein identification. Searches were performed against the SwissProt protein database for *Rattus norvergicus*. The search was performed including an MS tolerance of 30 ppm for precursor ions and 0.3 Da for fragment ions, as accepting up to two missed cleavages. Propionamide and methionine oxidation were set as variable modifications. The confidence level accepted for positive protein identification was $p<0.05$. Proteins were filtered accepting a false positive rate of 5%, determined with a reverse database. Furthermore, proteins identified with one peptide were manually validated when MS/MS spectra presented at least 4 successive amino acids covered by *b* or *y* fragmentations. The abundance of identified proteins (common to all groups) was estimated by calculating the exponentially modified protein abundance index (emPAI) [23] with the number of detected peptides divided by the number of observable peptides per protein, normalised by the theoretical number of peptides expected via *in silico* digestion. The observed peptides were unique parent ions, including those with two missed cleavages. Mean protein emPAI values were log2 transformed for protein ratio calculation.

Bioinformatics tools

Venny tool (http://bioinfogp.cnb.csic.es/tools/venny/index.html) was used to perform an integrative analysis of protein classes. Proteins were categorised by cellular component and molecular function according to Gene Ontology database (www.geneontology.org) annotation using the PANTHER classification system (http://www.pantherdb.org). Integrative analysis of CVAT proteome was performed with Cytoscape v3.6.1 and ClueGO+CluePedia [24], following these recommendations [25]. SecretomeP in conjunction with SignalP 4.1 was used to predict whether the secretory pathway is signal peptide-dependent (classic) or

signal peptide-independent and, hence, a non-classic pathway (SecretomeP 2.0).

Real-time PCR

For gene expression analyses in CVAT, RNA was extracted with TriPure (Roche). RT-PCR was performed with total RNA, followed by real-time PCR analyses using the SYBR Green method (Step-One™, Applied Biosystems). Standard curves were obtained for each gene correlating the cDNA quantities in graded dilutions from a randomly selected tissue sample with the respective threshold cycles (second derivative maximum method). GAPDH was used as internal control since its cDNA levels were similar in the studied groups. Results were normalised for GAPDH (set as arbitrary units, AU) and displayed relative to lean ZSF1 rats. Specific PCR primer pairs for the studied genes are listed in Table 1.

Table 1. List of primers for RT-PCR used in this study. F, sequence from sense strands; R, sequence from anti-sense strands

Genes	Primer sequence (5' → 3')	
UCP1	F: CCG AAA CTG TAC AGC GGT CT	R: GTC ATC AAG CCA GCC GAG AT
CIDEA	F: TGA CAT TCA TGG GGT TGC AGA	R: GGC CAG TTG TGA TGA CCA AGA
Adiponectin	F: GGG CTA CGG GCT GCT CTG A	R: TAT GGG GAA GGG GAC AAC AAT
PPARγ	F: AAG ACA TCC CGT TCA CAA G	R: CTA CTT TGA TCG CAC TTT GG
Leptin	F: TCT GCA GCA CGT TTT GGG AAG G	R: CCG CCA GGC AGA GGG TCA C
FABP4	F: AGA AGT GGG AGT TGG CTT CG	R: ACT CTC TGA CCG GAT GAC GA
Resistin	F: TGT GTC CCA TGG ATG AAG CC	R: AGT GAC GGT TGT GCC TTC TG
Visfatin	F: ACA AGA GAC TGC CGG CAT AG	R: CCG CTG GGA ACA GAA TAG CCT
Chemerin	F: CAG ACC AGC TGC CTG AAG AA	R: TGG GGT CCA GTT TGA TGC AG
Apelin	F: AAG GAA GGG GTG AGG AGA AA	R: TCA TGG GTT CCT CTC CTT TG
GAPDH	F: TGG CCT TCC GTG TTC CTA CC C	R: CCG CCT GCT TCA CCA CCT TCT

Protein analysis by Western Blot

CVAT and left ventricular samples were homogenized in RIPA buffer (150 mM NaCl, 1% IGEPAL CA-630, 0.5% sodium deoxycholate, 0.1% SDS, 50 mM Tris, pH 8.0; Sigma-Aldrich, R0278), and protein concentration was determined based on the method of Bradford (Bio-Rad Protein Assay, 500-0006). Forty micrograms (40 µg) of protein of each sample was prepared with Laemmli buffer (1 M Tris-HCl pH 6.8, 10% SDS, 20% glycerol, 0.004% bromophenol blue, 20% 2-mercaptoethanol) randomly loaded and separated by SDS-PAGE (Mini-PROTEAN Tetra Cell, Bio-Rad). After transferring to a nitrocellulose membrane (Bio-Rad 1620115 and 1620112) and blocking with 5% BSA (w/v; A2058, Sigma-Aldrich) in TBS-0.5% Tween (Tris-buffered saline-Tween 20). The membranes were cut and incubated with primary antibody overnight at 4°C (UCP-1, Abcam ab23841; mTOR, Cell Signalling 2972 and p-mTOR, Cell Signalling 2971). Finally, membranes were incubated for an hour at room temperature with secondary antibody (IRDye 680LT, LI-COR). The signal was detected by an image acquisition system (Odyssey Infrared Imaging System LI-COR Biosciences at 700 or 800 nm) and the image acquired before signal saturation. The signal was normalised to total protein density (Ponceau S (Sigma-Aldrich P7170)) as previously described [26].

Statistical analysis

Values are expressed as mean ± standard error of mean (SEM). Single comparisons were assessed by an unpaired Student t-test. One-way ANOVA test was used for comparison among groups. In all analysis, $p<0.05$ was considered statistically significant. Statistical analysis was performed using GraphPad (version 7).

Results

ZSF1 Obese Display Metabolic Syndrome And Diastolic Dysfunction Consistent With A Phenotype Of HFPEF

Obese rats presented higher body weight than lean rats, and showed hypertrophic hearts, with a significant increase in heart weight normalised to tibia length (Table 2). As for body composition, obese rats presented a significant increase in lungs, perigonadal, perirenal and cardiac fat pads weight (Fig. 1) compared to lean ZSF1 group (Table 2 and Fig. 2). Despite the obesity, obese ZSF1 presented muscle atrophy as denoted by the lower gastrocnemius/tibia length.

Regarding metabolic characterisation, obese rats showed hyperlipidaemia, impaired glucose tolerance, insulin resistance and hyperglycaemia, consistent with the diagnosis of metabolic syndrome (Table 2).

Consistent with our previous reports [12-15], obese rats presented an HFpEF phenotype. Thus, compared to the lean, the obese ZSF1 group displayed: 1) lung congestion; 2) normal left ventricle (LV) systolic function, as supported by similar cardiac index (CI) and ejection fraction (EF); 3) significant diastolic abnormalities, namely higher filling pressures, as confirmed by an increase in E/E' and 4) increased left atrium area (LAA) (Table 2). Furthermore, CVAT weight correlated significantly with diastolic dysfunction, reinforcing the possible link between CVAT and the clinical features of HFpEF (Fig. 2D-2F).

Table 2. Morphometric, metabolic and echocardiographic data. TL, tibial length; OGT, oral glucose test; IR, insulin resistance; AUC, area under curve; EF, ejection fraction; E/E', ratio of transmitral Doppler early filling velocity to tissue Doppler early diastolic mitral anular velocity; E/A, ratio of the early (E) to late (A) mitral filling velocities; LAA, left atrium area; CI, cardiac índex; HR, heart rate; LV, left ventricle. The values are given as means ± SEM

Parameters	Lean	Obese	P Value
Morphometric data			
Body weight, g	457.7 ± 14.1	594.1 ± 8.5	<0.001
TL, mm	41.2 ± 0.4	40.6 ± 0.3	0.28
Heart/TL, mg.mm^{-1}	35.9 ± 1.4	41.6 ± 1.6	0.02
Lung/TL, mg.mm^{-1}	42.9 ± 1.5	59.4 ± 7.1	0.03
Gastrocnemius/TL, mg.mm^{-1}	60.4 ± 2.0	50.7 ± 2.2	0.006
Metabolic data			
Glycaemia level, mg.dL^{-1}	73 ± 5	134 ± 10	<0.001
OGT AUC, mg.dL^{-1}.h^{-1}	82 ± 12	171 ± 15	<0.001
IR AUC, mg.dL^{-1}.h^{-1}	50 ± 6	139 ± 10	0.006
Cholesterol, mg.dL^{-1}	47 ± 2	130 ± 14	<0.001
Echocardiographic data			
EF, %	73.4 ± 2.0	74.2 ± 1.7	0.79
CI, mL.min^{-1}.cm^{-2}	199 ± 12	213 ± 11	0.43
HR, bpm	315 ± 10	318 ± 9	0.84
LV mass, mg	573 ± 27	773 ± 27	<0.001
E/E'	12.07 ± 0.38	16.16 ± 0.47	<0.001
E/A	1.54 ± 0.08	1.36 ± 0.07	0.16
LAA, mm^2	2.62 ± 0.13	3.50 ± 0.05	<0.001
MPI, Tei	0.65 ± 0.02	0.63 ± 0.03	0.52

Characterisation Of Cardiac Visceral Adipose Tissue

Proteomic analysis.

Functional protein categorisation and integrative analysis with Cytoscape: The CVAT proteome differences between lean and obese ZSF1 were assessed by GeLC-MS/MS. SDS-PAGE band profile did not highlight inter-individual biological variations (Supplementary Fig. S1 – for all supplemental material see www.cellphysiolbiochem.com). Whole gel bands' analysis by LC-MS/MS retrieved 259 distinct proteins (Supplementary Table S1).

A Venn diagram displays the unique and commonly expressed CVAT proteins from lean and obese groups (Fig. 3A). From all proteins identified in CVAT, only 88 were common to lean and obese rats (Supplementary Table S2). Regarding the unique proteins, seventy-three and ninety-eight proteins were exclusively identified in lean rats and obese rats, respectively (Supplementary Table S2).

Overall, the identified proteins are involved in different biological processes such as metabolic and cellular processes and are mostly found in cell parts and organelles (Supplementary Fig. S2). Concerning molecular function, an enrichment of proteins with catalytic and binding activity was evident (Supplementary Fig. S2). Enrichment analysis also highlighted a higher prevalence of proteins associated with cellular components organization or biogenesis, biological regulation, structural molecule activity and binding and a lower representation of membrane proteins and those with catalytic activity in the obese group.

Regarding the common proteins, normalised abundance analysis evidenced the fibrinogen beta chain (FIBB), heterogeneous nuclear ribonucleoprotein A2/B1 (ROA2), alpha-1-macroglobulin (A1M), alpha-1-antiproteinase (A1AT) and hemopexin (HEMO) as the most abundant proteins in CVAT from obese rats. Contrarily, 2-oxoglutarate dehydrogenase (ODO1), aconitate hydratase (ACON), electron transfer flavoprotein subunit alpha (ETFA),

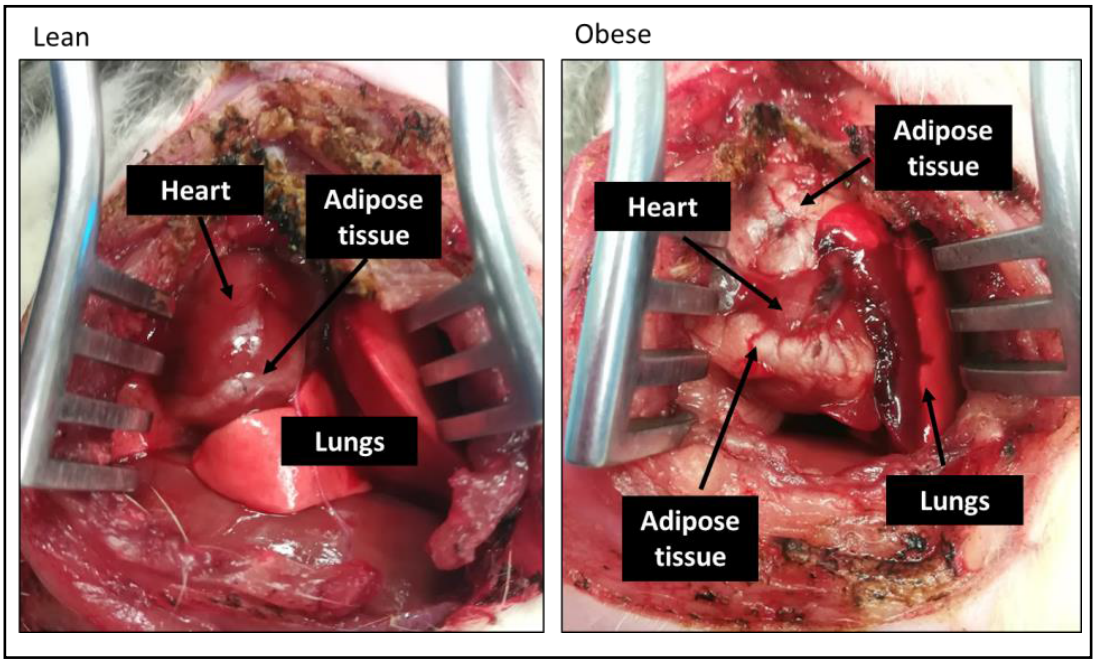

Fig. 1. Representative images of the thoracic cavity of lean and obese ZSF1 before euthanasia. Although not visible, the pericardial membranes were still intact in both pictures and CVAT was collected from the pericardial cavity.

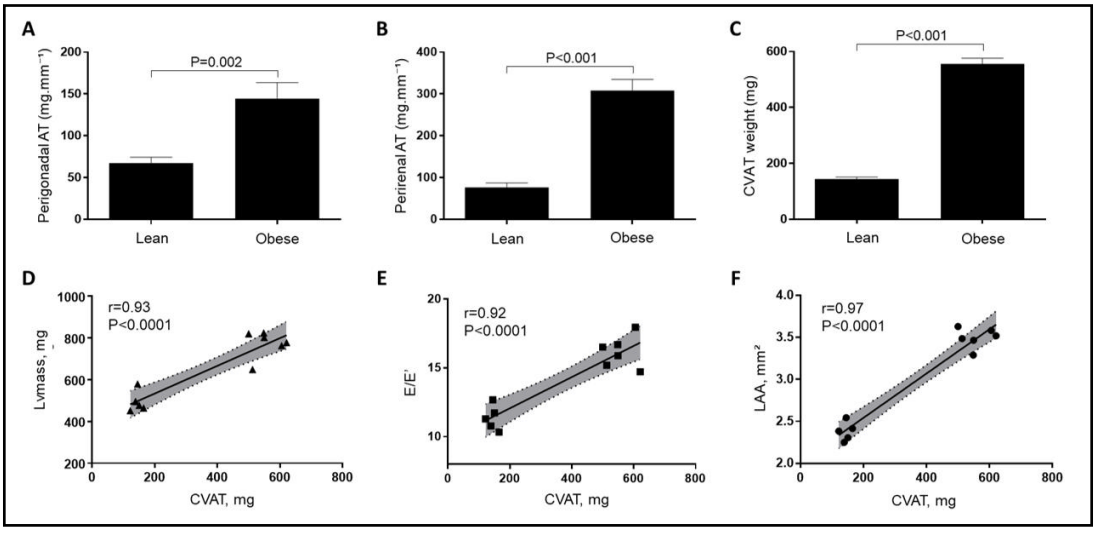

Fig. 2. Adipose tissue depots weights in obese and lean ZSF1: A - Perigonadal adipose tissue; B - Perirenal adipose tissue; C - Cardiac visceral adipose tissue (CVAT). Correlations between cardiac visceral adipose tissue weight and: D – left ventricle mass; E – ratio of transmitral Doppler early filling velocity to tissue Doppler early diastolic mitral annular velocity (E/E'); F – left atrium area (LAA). The values are given as means ± SEM. n = 8-10 animals per group.

mitochondrial brown fat uncoupling protein 1 (UCP1) and cytochrome b5 (CYB5) were the most abundant proteins in CVAT from lean rats, thus downregulated in obese ZSF1 (Fig. 4 and Supplementary Table S2).

Protein-protein interactions analysis considering unique proteins and the ones significantly different between groups (emPAI ratio >1.25 or <-1.25, Fig. 3B) highlighted key biological processes in CVAT from obese ZSF1, namely "regulation of heterotypic cell-

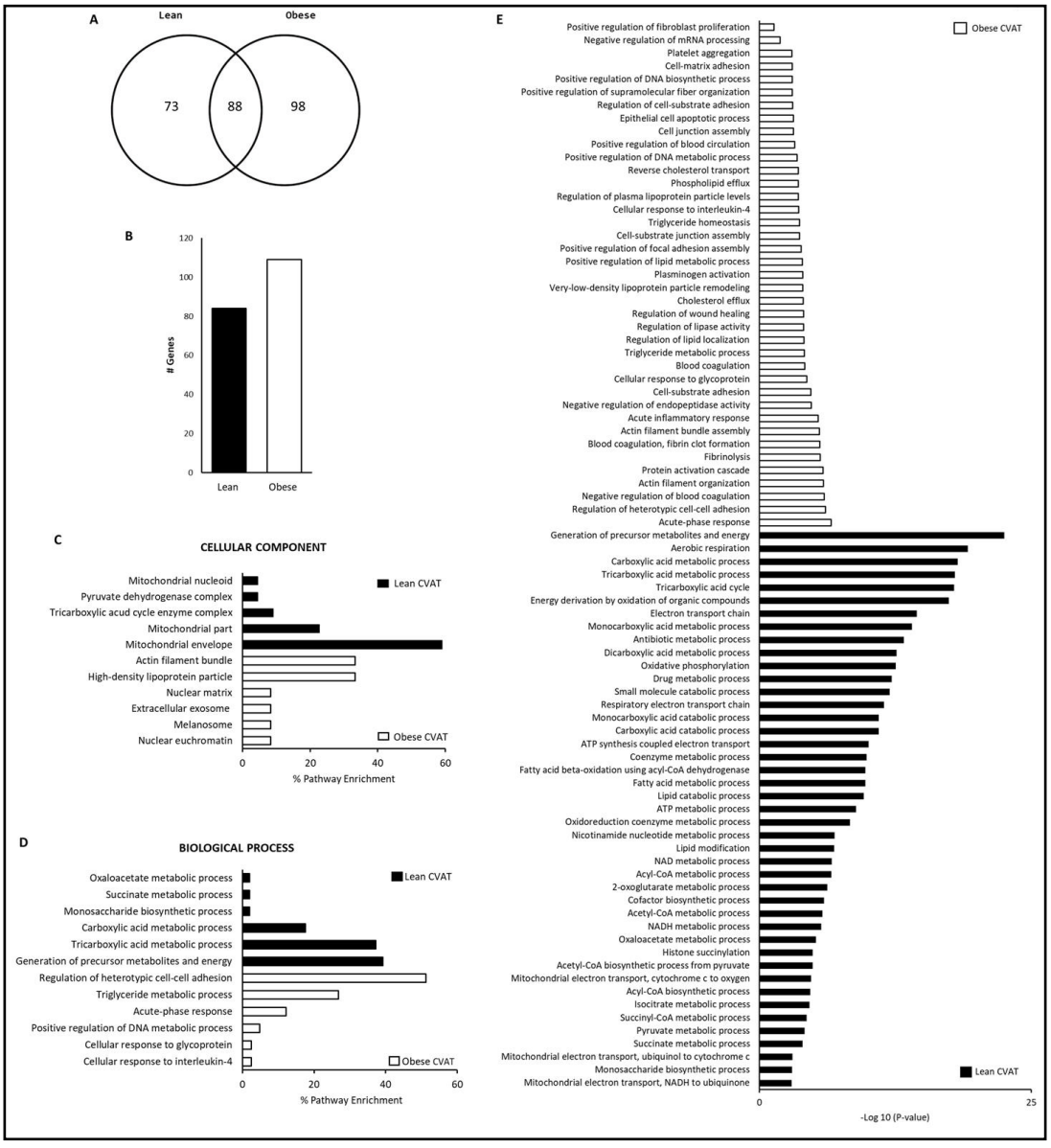

Fig. 3. Proteomics identification of protein and pathways. A - Venn diagram depicting the number of unique and overlapping genes between the two groups. B - Bar graph representation considering unique and most significantly different proteins in Lean and Obese CVAT. C - ClueGo and CluePedia analysis of cellular components considering unique and the most significantly different proteins. D - ClueGo and CluePedia analysis of biological process considering unique and the most significantly different proteins. E - Enrichment analysis of biological process pathways among lean and obese CVAT. The horizontal axis presents the -log10 of P-value), whereas the vertical axis presents the pathway name. The larger value of the horizontal axis suggests a more significantly enriched pathway in lean and obese CVAT.

cell adhesion", "triglyceride metabolic process", "acute-phase response", "positive regulation of DNA metabolic process", "cellular response to glycoprotein" and "cellular response to interleukin-4". In contrast, "generation of precursor metabolites and energy", "tricarboxylic acid metabolic process", "carboxylic acid metabolic process", "monosaccharide biosynthetic process", "succinate metabolic process" and "oxaloacetate metabolic process" were noted as the main classifications for lean CVAT (Fig. 3D and Supplementary Fig. 3). Moreover, Fig. 3E identified pathways markedly enriched in biological processes in lean and obese CVAT.

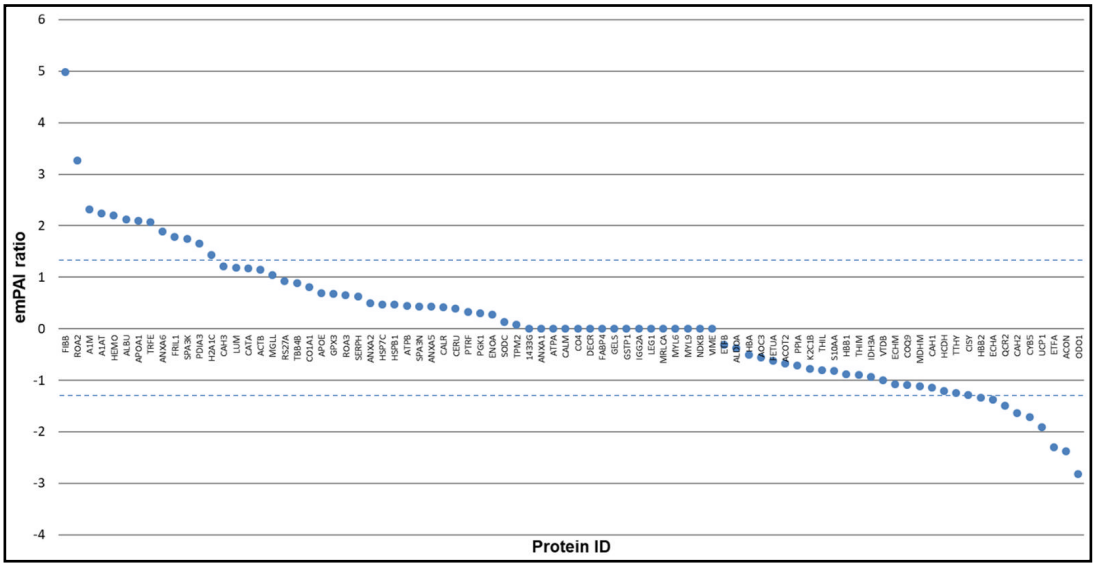

Fig. 4. Distribution of normalised emPAI values of CVAT proteins from obese and lean ZSF1 highlighting differences in protein expression. Entry name correlates protein name at Supplemental Table 3. Values above zero correspond to proteins up-regulated in obese animals. Values below zero correspond to proteins down-regulated in obese animals.

Cellular component classification revealed that many lean CVAT proteins were assigned to "mitochondrial envelope" and "mitochondrial part". In contrast, obese CVAT proteins were associated with "actin filament bundle" and "high-density lipoprotein particle" (Fig. 3C).

Predictions of putative secreted proteins: In order to add new insights on CVAT interactions with other targets, SignalP (v4.1) and SecretomeP (v2.0) bioinformatics analyses of all identified proteins were performed to search for putative secreted proteins. SignalP predicts classically secreted proteins based on the presence of a signal peptide, whilst SecretomeP predicts non-classical secreted proteins from exosomes and microvesicles. From the 259 proteins identified, 68 were predicted as classically and 86 non-classically secreted (Supplementary Table S3). Looking at the unique and differentially expressed proteins that are potentially secreted by obese CVAT, 38 classically and 33 non-classically secreted proteins were identified whereas in lean rats, 15 classically and 25 non-classically secreted proteins were annotated (Supplementary Table S3). Functional enrichment analysis considering classical secreted proteins alone highlighted "negative regulation of blood coagulation", "protein activation cascade" and "regulation of lipoprotein lipase activity" as the most prevalent biological processes in obese rats and "fatty acid catabolic process" and "tricarboxylic acid cycle" in lean rats (Fig. 5A and Supplementary Fig. S4). In turn, functional analysis of non-classically secreted proteins evidenced again a marked up-regulation of "negative regulation of blood coagulation" in obese and of "electron transport chain" and "fatty acid beta-oxidation using acyl-CoA dehydrogenase" in lean rats (Fig. 5B and Supplementary Fig. S5). The latter finding is corroborated by the negative correlation between CVAT weight and mitochondrial functional parameters of LV from lean and obese rats (Supplementary Fig. S6).

Cardiac visceral adipose tissue alterations. Following the proteomic findings, we studied the CVAT in order to validate the observed alterations. The obese CVAT presented hypertrophied adipocytes compared to lean CVAT (Fig. 6A/B). This observation suggests that CVAT becomes a site of deranged adipogenesis as a consequence of obesity/metabolic syndrome. Thus, considering our results, we decided to analyse the expression levels of some adipocyte-type-specific markers and pro-inflammatory adipokines related to inflammation and cardiac remodelling. As shown in Fig. 6D/E, we confirmed that UCP-1 expression was

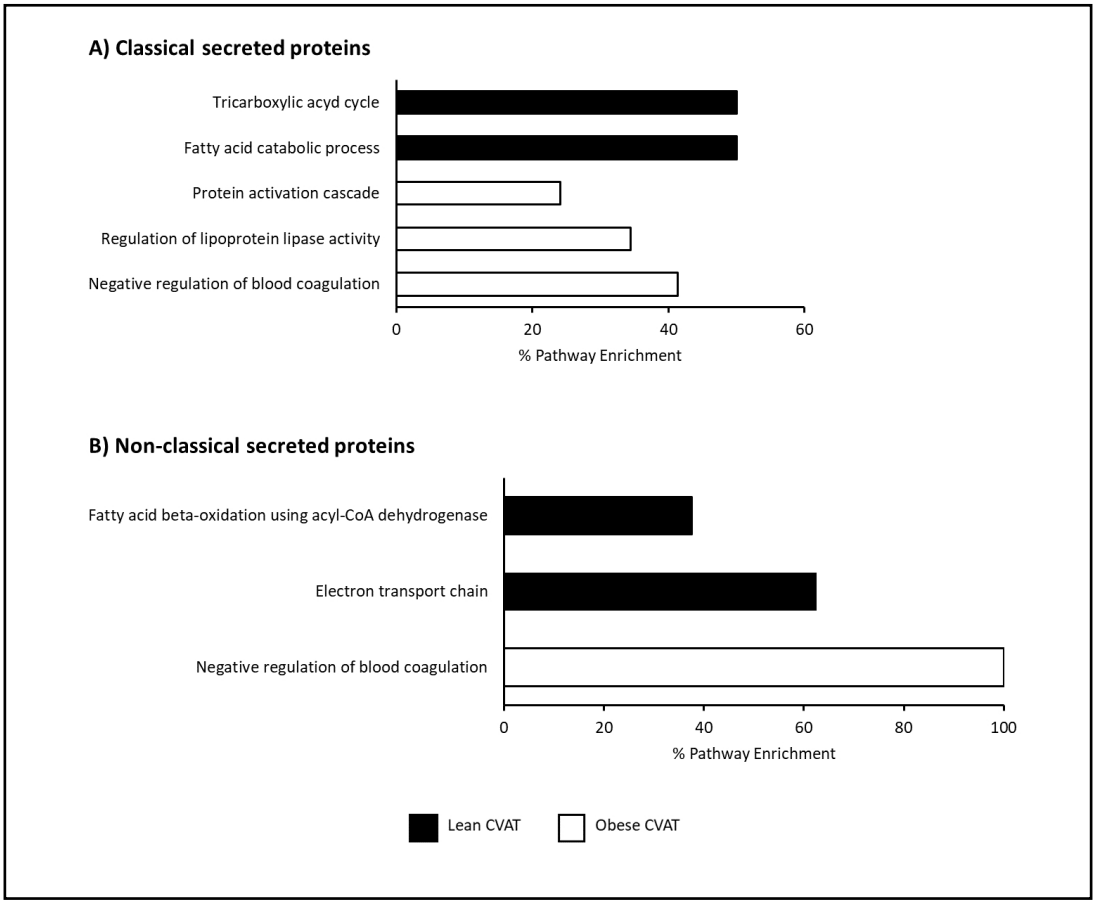

Fig. 5. ClueGo and CluePedia analysis of cellular component considering unique and common proteins with the prediction of classically secreted proteins (A) and non-classically secreted proteins (B) in CVAT of obese and lean rats.

higher in CVAT samples of lean compared with obese. Moreover, lean CVAT showed an increased expression of a marker of brown adipose tissue (CIDEA, Fig. 6F).

Conversely, obese CVAT presented a higher expression of PPAR-γ and adiponectin, which are markers for white adipose tissue (Fig. 6G/6C). Regarding pro-inflammatory adipokines, the results showed overexpression of leptin, FABP4, visfatin, chemerin and apelin in obese compared to lean CVAT (Fig. 6H – 6M). Accordingly, CVAT weight correlates with the expression of adipokines, confirming that remodelling of adipose tissue in obesity promotes a higher expression of pro-inflammatory adipokines (Supplementary Fig. S7). To elucidate the cross-talk of these adipokines with the heart, we evaluated mTOR activity in LV from both groups, an important regulator of cardiac hypertrophy. We confirmed a higher activity of mTOR in the obese group compared with the lean group, which is also positively correlated with the expression of CVAT adipokines (Supplementary Fig. S8).

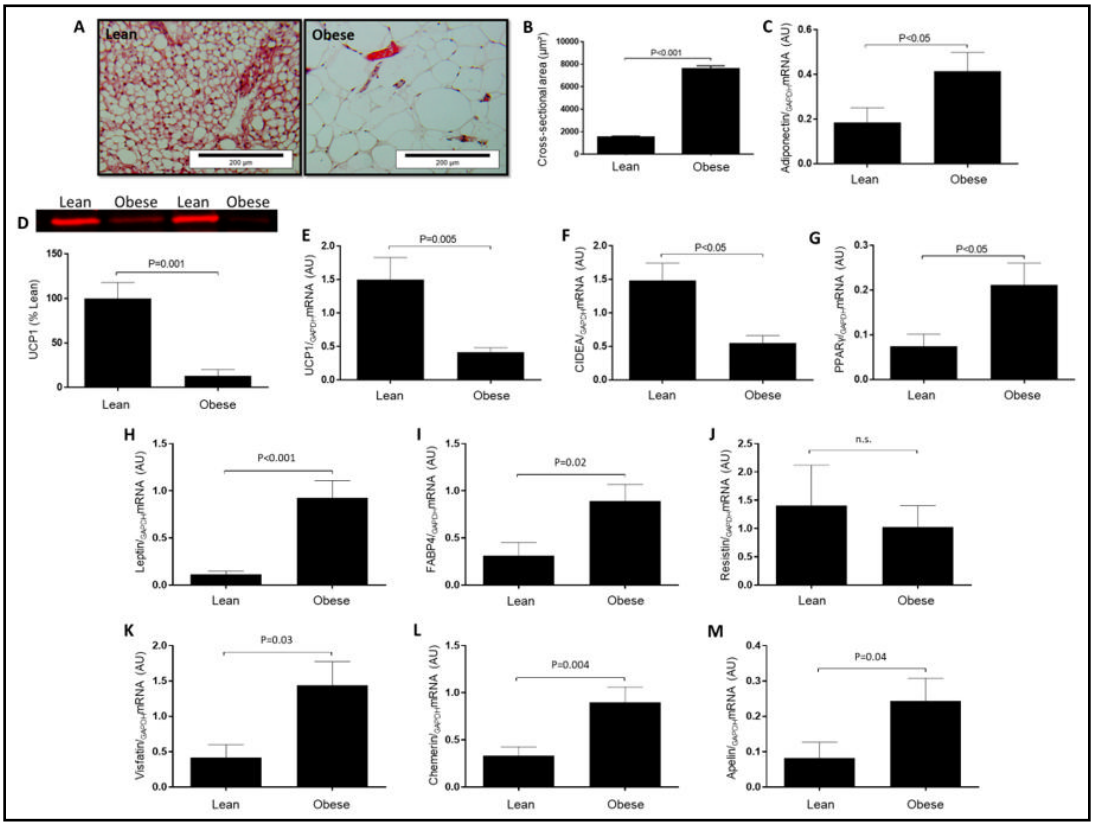

Fig. 6. Representative histological images of Lean and Obese CVAT (A) and cross-sectional area of adipocytes (μm^2) (B). Protein expression of UCP1 (D) and mRNA expression of UCP1 (E), adiponectin (C), CIDEA (F), PPARγ (G), leptin (A), FABP4 (B), resistin (C), visfatin (D), chemerin (E), apelin (F) in CVAT from lean and obese ZSF1. The values are given as means ± SEM. n = 6-8 animals per group.

Conditioned Media Derived From CVAT Of Obese ZSF1 Damages Cardiac Structure And Function

Considering the proximity between CVAT and heart, we tried to evaluate the endocrine role of lean and obese CVAT by using conditioned media derived from lean and obese CVAT in cardiac organo-cultures and cardiomyocytes.

CVAT from obese ZSF1 induces cardiac hypertrophy and fibrosis. Cardiac organo-cultures incubated for 24 hours with CM-obese showed higher cardiomyocyte cross-sectional area in ventricular slices when compared to ventricular slices treated with CM-lean and control (minimum medium) (Fig. 7A). Likewise, fibrosis was significantly increased in slices treated with CM-obese compared to CM-lean and control (minimum medium) (Fig. 7B).

CVAT from obese ZSF1 decreases cardiomyocytes viability. Adult rat cardiomyocytes were incubated with conditioned media and were analysed for cardiomyocyte viability. Fig. 7D showed a significant reduction in cell viability as soon as 3 hours of incubation with CM-obese compared to CM-lean and to control.

Discussion

The present study describes the main differences between CVAT phenotype and proteome between obese and lean control rats and reveals the myocardial impact of CVAT. We described, for the first time, the direct myocardial effects of obese-derived CVAT conditioned media as noted by increased hypertrophy and fibrosis, as well as, by decreased cardiomyocytes viability. A subsequent bioinformatics approach highlighted the most

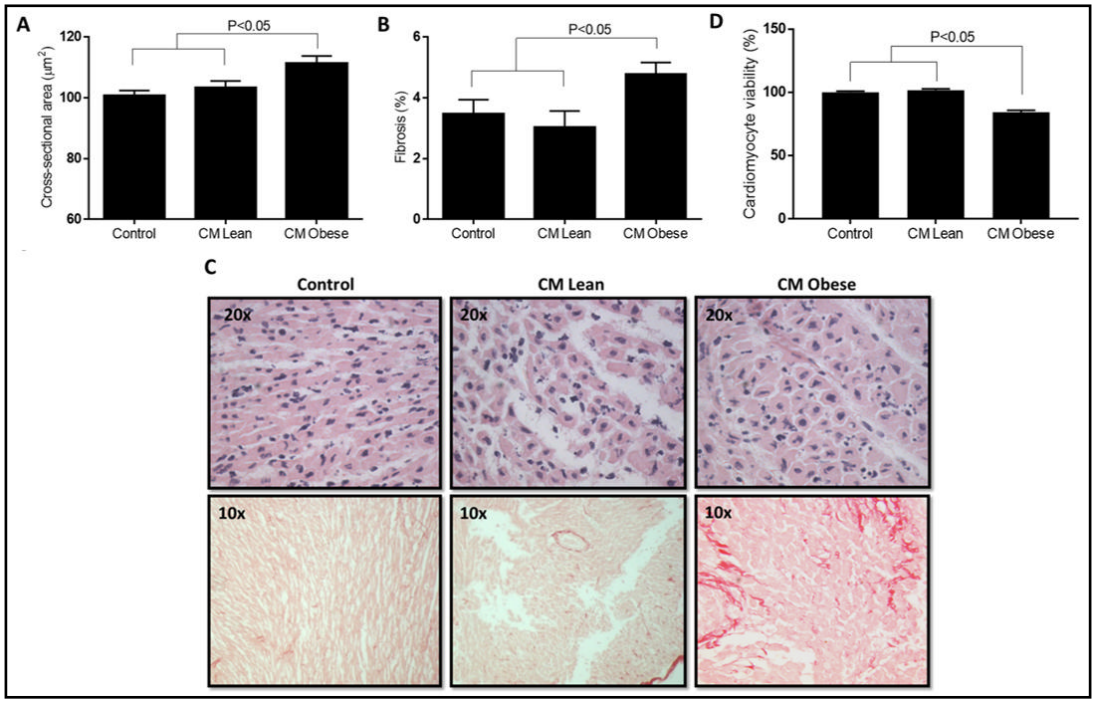

Fig. 7. Cardiac changes promoted by CVAT-derived conditioned media. A - Cross-sectional area of cardiomyocytes (μm^2) assessed in ventricular organo-cultures 24 hours after stimulation with conditioned media (CM) from Lean (CM-lean) and obese (CM-lean) animals or minimum medium (control). B - Fibrosis (%) assessed in ventricular organo-cultures 24 hours after stimulation with CM-lean, CM-obese animals or minimum medium (control). C - Representative images of cross-sectional area of cardiomyocytes and fibrosis. D - Cardiomyocyte viability after stimulation for 3 hours with CM-lean, CM-obese animals or minimum medium (control). The values are given as means ± SEM.

important signalling pathways that were altered in the obese group. This work provides relevant evidence regarding the deleterious impact of CVAT from obese individuals in the myocardium and provides evidence of how obesity and other comorbidities participate in metabolic and structural alterations of CVAT.

ZSF1 obese rats have been considered a robust model of HFpEF associated with cardiometabolic syndrome [12-15]. Both obese and lean rats are hypertensive and present normal systolic function. However, obese rats exhibit diastolic abnormalities displaying increased stiffness and impaired relaxation, with an impressive accumulation of fat tissue depots, including CVAT. Therefore, we hypothesized that expanded CVAT depots could have a direct myocardial effect. Indeed, the accumulation of cardiac adipose tissue closely associates with cardiac diastolic abnormalities and has been described in obesity, showing that patients with obesity-related HFpEF have increased epicardial fat thickness [27]. Abundant CVAT can be found in larger mammals and humans [28], but little or no CVAT is present in rats, which can explain why CVAT has been poorly studied in small animal models when compared with others fat depots (subcutaneous or visceral) [28].

Obese CVAT accumulates large amounts of lipids, promoting constant and dynamic remodelling in adipose tissue in response to metabolic alterations observed in these rats. This can induce dysregulation of adipose tissue derived-adipokines, cytokines, hormones and metabolites. Our study corroborates this notion, as higher expression of pro-inflammatory adipokines was found in obese CVAT. These molecules can participate through endocrine, paracrine or autocrine mechanisms in a great variety of physiological and/or pathophysiological processes, being main contributors to a systemic pro-inflammatory state [12]. In fact, patients with obesity-related HFpEF exhibit a biological shift toward the synthesis of pro-inflammatory cytokines in epicardial adipose tissue [27, 29]. The

mechanisms by which pro-inflammatory adipokines and cytokines mediates cardiovascular disease progression in obesity has been described on the different cardiac cell types [30]. However, few studies have analysed the effects of adipose tissue secretome on cardiac function.

We have shown that besides CVAT alterations, the secretome delivered to the conditioned media was able to directly induce fibrosis, cardiomyocyte hypertrophy and apoptosis. Regarding to cellular metabolism, assessed by resazurin-test, we performed viability tests in cardiomyocytes exposed to CM-obese and noticed a significant reduction in the number of cells responding to external pacing, meaning that among "survivor" cardiomyocytes only a few were still capable of contracting and, thus, could be considered as functional cells (data not shown). Alterations in cardiomyocyte metabolism can contribute to cardiac pathologies, including HFpEF [31, 32]. Moreover, cardiomyocytes apoptosis is a component of cardiac remodelling that can contribute to heart failure [33]. Our study further supports other studies, in which a high-calorie "Western" diet-induced obesity was capable of augmenting cardiac apoptosis and mitochondrial dysfunction, demonstrating that metabolic products of obesity, such as pro-inflammatory adipokines/cytokines, can be involved in the development of cardiovascular diseases [30, 34-36].

Considering CVAT changes and its impact on the myocardium, we subsequently analysed and compared the proteome of lean and obese CVAT. Our results showed a different protein profile, as confirmed by the number of the unique proteins that were identified. An integrative analysis was carried out to get an insight into the most significant biological processes regulated in lean and obese CVAT. Indeed, in obese CVAT a significant up-regulation of triglyceride metabolic processes and of heterotypic cell-cell adhesion was observed. Obesity develops when energy production/intake exceeds energy expenditure and the balance between energy supply and demand is disturbed. In such case, adipose tissue stores the excess of energy in the form of triglycerides [37]. When adipocyte size is greatly increased, as found in this study, there is a lipid "spill-over" that contribute to hyperlipidaemia. The connective content of adipose tissue increases intensively in order to maintain the structural integrity of adipocytes in obesity, and subsequently, adipocytes share their microenvironment with multiple cell types that interact to coordinate adipose functions [38, 39]. Therefore, cell-cell adhesion is essential for the regeneration, expansion and maintenance of adipose tissue [39].

Contrarily, the lean CVAT reveals itself as a metabolic active fat depot, rich in mitochondrial proteins mainly involved in the major mitochondrial functions, such as aerobic respiration, tricarboxylic acid cycle or fatty acid catabolic process. The emPAI analysis revealed the presence of mitochondrial brown fat uncoupling protein 1 (UCP-1) significantly up-regulated. As a specific brown adipose tissue marker, UCP-1 up-regulation suggests a brown adipose tissue-like phenotype in lean CVAT. Brown adipose tissue is a peculiar adipose tissue, which presents a higher content of mitochondria characterised by an increased expression of UCP-1 [40]. The typical multilocular lipid stores in brown adipose tissue provide a rapid source of fatty acids for activated mitochondria that rapidly produce adenosine triphosphate (ATP) and dissipate it as heat [41]. A brown adipose tissue signature has been described by some authors in human cardiac adipose tissue, suggesting that this subtype can be important in maintaining myocardial temperature by heating and conferring a survival advantage by protecting the heart during hypothermia, ischaemia or hypoxia [42]. Under normal conditions or metabolically healthy individuals, adipocytes in CVAT behave as expected from those found in brown adipose tissue, but when metabolic syndrome is associated with obesity, CVAT resembles more with white adipose tissue [27].

The proximity between CVAT and the myocardium favours potential interactions between these tissues [27, 43]. The analysis of putative secreted proteins reveals the proteins that can be potentially released by CVAT. Network analysis with these proteins showed that lean and obese CVAT might influence cardiac metabolism. The proteins potentially secreted by obese CVAT are involved in negative regulation of blood coagulation or in the activity of lipoprotein lipase, that is crucial to break down fat in the form of triglycerides, and contribute for the

accumulation of lipids in organs. In contrast, the proteins theoretically secreted by lean CVAT can contribute to the maintenance of cardiac mitochondrial function, as they participate in processes such as electron transport chain, fatty acid catabolic process or tricarboxylic cycle, which are crucial processes to energy production. In fact, the myocardium has high energy requirements that are evidenced by the high rates of ATP synthesis. Therefore, the heart has a higher degree of metabolic flexibility, which is demonstrated by its ability to use various energy substrates to generate ATP in several conditions [44].

Previous reports have documented the impact that other comorbidities or other fat depots might have on the myocardium [12]. In our study, we have shown that lean and obese CVAT have different proteomic signatures, demonstrating that CVAT is susceptible to metabolic modulation with obesity, and can directly affect the heart inducing fibrosis, cardiomyocyte hypertrophy and apoptosis as well as significantly affect important myocardial metabolic processes.

Conclusion

We provide evidence that CVAT suffered a brown-to-white differentiation upon the influence of obesity-related comorbidities. CVAT, through its significant physiological alterations in obesity, could be an important determinant for cardiac alterations in a paracrine manner. Therefore, CVAT can no longer be disregarded as a deleterious piece of HFpEF complexity. Instead, research directed towards unravelling the interaction between CVAT and the heart urges as this fat depot might represent an important player of HFpEF induced by metabolic disorders.

Acknowledgements

We thank Prof. Carla Marques for her technical input in the organo-culture model. We thank Sara Leite and Dulce Fontoura for their support with the animal model maintenance. The authors thank Fábio Trindade for critically reading the paper.

Statement of Ethics

All the procedures in this work followed the recommendations of the Guide for the Care and Use of Laboratory Animals, published by the US National Institutes of Health (NIH Publication No. 85-23, Revised 2011) and were certified by the Portuguese Veterinary Governmental Authorities and by the ethical committee of the institution. Only trained researchers, certified with a Laboratory Animal Science course according to the Federation of European Laboratory Animal Science Associations, performed animal handling and procedures.

Funding Sources

This project is supported by Fundo Europeu de Desenvolvimento Regional (FEDER) through Compete 2020 – Programa Operacional Competitividade E Internacionalização (POCI), the project DOCNET (norte-01-0145-feder-000003), supported by Norte Portugal regional operational programme (norte 2020), under the Portugal 2020 partnership agreement, through the European Regional Development Fund (ERDF), the project NETDIAMOND (POCI-01-0145-FEDER-016385), supported by European Structural And Investment Funds, Lisbon's regional operational program 2020 and supported by the Cardiovascular R&D Center, financed by national funds through FCT - Fundação para a Ciência e Tecnologia, I.P., under the scope of the projects UID/IC/00051/2019 and UIDP/00051/2020. Glória Conceição is supported by the PhD grant Program (Norte-08-5369-FSE-000024), financed by Norte Portugal Regional Operational Programme (NORTE 2020), through the CCDRN, PORTUGAL 2020 and the European Social Fund (ESF).

Author Contributions

GC, NG, ALM, RV and IFP generated the hypothesis, designed the experiments and wrote the manuscript. GC, JM, RF, RV and IFP analysed and discussed the data.

Disclosure Statement

The authors have no conflicts of interest to declare.

References

1 Borlaug BA, Paulus WJ: Heart failure with preserved ejection fraction: pathophysiology, diagnosis, and treatment. Eur J Heart 2011;32:670-679.
2 Conceicao G, Heinonen I, Lourenco AP, Duncker DJ, Falcao-Pires I: Animal models of heart failure with preserved ejection fraction. Neth Heart J 2016;24:275-286.
3 Hubert HB, Feinleib M, McNamara PM, Castelli WP: Obesity as an independent risk factor for cardiovascular disease: a 26-year follow-up of participants in the Framingham Heart Study. Circulation 1983;67:968-977.
4 Lavie CJ, Milani RV, Ventura HO: Obesity and cardiovascular disease: risk factor, paradox, and impact of weight loss. J Am Coll Cardiol 2009;53:1925-1932.
5 Guglielmi V, Sbraccia P: Epicardial adipose tissue: at the heart of the obesity complications. Acta Diabetol 2017;54:805-812.
6 Rabkin SW: Epicardial fat: properties, function and relationship to obesity. Obes Rev 2007;8:253-261.
7 Selthofer-Relatic K, Bosnjak I: Myocardial fat as a part of cardiac visceral adipose tissue: physiological and pathophysiological view. J Endocrinol Invest 2015;38:933-939.
8 Sacks HS, Fain JN: Human epicardial adipose tissue: a review. Am Heart J 2007;153:907-917.
9 Alexopoulos N, McLean DS, Janik M, Arepalli CD, Stillman AE, Raggi P: Epicardial adipose tissue and coronary artery plaque characteristics. Atherosclerosis 2010;210:150-154.
10 Mahabadi AA, Massaro JM, Rosito GA, Levy D, Murabito JM, Wolf PA, O'Donnell CJ, Fox CS, Hoffmann U: Association of pericardial fat, intrathoracic fat, and visceral abdominal fat with cardiovascular disease burden: the Framingham Heart Study. Eur Heart J 2009;30:850-856.
11 Fox CS, Gona P, Hoffmann U, Porter SA, Salton CJ, Massaro JM, Levy D, Larson MG, D'Agostino RB Sr., O'Donnell CJ, Manning WJ: Pericardial fat, intrathoracic fat, and measures of left ventricular structure and function: the Framingham Heart Study. Circulation 2009;119:1586-1591.
12 Hamdani N, Franssen C, Lourenco A, Falcao-Pires I, Fontoura D, Leite S, Plettig L, Lopez B, Ottenheijm CA, Becher PM, Gonzalez A, Tschope C, Diez J, Linke WA, Leite-Moreira AF, Paulus WJ: Myocardial titin hypophosphorylation importantly contributes to heart failure with preserved ejection fraction in a rat metabolic risk model. Circ Heart Fail 2013;6:1239-1249.
13 Leite S, Rodrigues S, Tavares-Silva M, Oliveira-Pinto J, Alaa M, Abdellatif M, Fontoura D, Falcao-Pires I, Gillebert TC, Leite-Moreira AF, Lourenco AP: Afterload-induced diastolic dysfunction contributes to high filling pressures in experimental heart failure with preserved ejection fraction. Am J Physiol Heart Circ Physiol 2015;309:H1648-1654.
14 van Dijk CG, Oosterhuis NR, Xu YJ, Brandt M, Paulus WJ, van Heerebeek L, Duncker DJ, Verhaar MC, Fontoura D, Lourenco AP, Leite-Moreira AF, Falcao-Pires I, Joles JA, Cheng C: Distinct Endothelial Cell Responses in the Heart and Kidney Microvasculature Characterize the Progression of Heart Failure With Preserved Ejection Fraction in the Obese ZSF1 Rat With Cardiorenal Metabolic Syndrome. Circ Heart Fail 2016;9:e002760.
15 Leite S, Oliveira-Pinto J, Tavares-Silva M, Abdellatif M, Fontoura D, Falcao-Pires I, Leite-Moreira AF, Lourenco AP: Echocardiography and invasive hemodynamics during stress testing for diagnosis of heart failure with preserved ejection fraction: an experimental study. Am J Physiol Heart Circ Physiol 2015;308:H1556-1563.

16 Lourenco AP, Leite-Moreira AF, Balligand JL, Bauersachs J, Dawson D, de Boer RA, de Windt LJ, Falcao-Pires I, Fontes-Carvalho R, Franz S, Giacca M, Hilfiker-Kleiner D, Hirsch E, Maack C, Mayr M, Pieske B, Thum T, Tocchetti CG, Brutsaert DL, Heymans S: An integrative translational approach to study heart failure with preserved ejection fraction: a position paper from the Working Group on Myocardial Function of the European Society of Cardiology. Eur J Heart Fail 2018;20:216-227.
17 Habeler W, Peschanski M, Monville C: Organotypic heart slices for cell transplantation and physiological studies. Organogenesis 2009;5:62-66.
18 Kaestner L, Scholz A, Hammer K, Vecerdea A, Ruppenthal S, Lipp P: Isolation and genetic manipulation of adult cardiac myocytes for confocal imaging. J Vis Exp 2009; DOI: 10.3791/1433.
19 Fowler ED, Benoist D, Drinkhill MJ, Stones R, Helmes M, Wust RC, Stienen GJ, Steele DS, White E: Decreased creatine kinase is linked to diastolic dysfunction in rats with right heart failure induced by pulmonary artery hypertension. J Mol Cell Cardiol 2015;86:1-8.
20 van Deel ED, Najafi A, Fontoura D, Valent E, Goebel M, Kardux K, Falcao-Pires I, van der Velden J: In vitro model to study the effects of matrix stiffening on Ca(2+) handling and myofilament function in isolated adult rat cardiomyocytes. J Physiol 2017;595:4597-4610.
21 Rosa CM, Gimenes R, Campos DH, Guirado GN, Gimenes C, Fernandes AA, Cicogna AC, Queiroz RM, Falcao-Pires I, Miranda-Silva D, Rodrigues P, Laurindo FR, Fernandes DC, Correa CR, Okoshi MP, Okoshi K: Apocynin influence on oxidative stress and cardiac remodeling of spontaneously hypertensive rats with diabetes mellitus. Cardiovasc Diabetol 2016;15:126.
22 Laemmli UK: Cleavage of structural proteins during the assembly of the head of bacteriophage T4. Nature 1970;227:680-685.
23 Ishihama Y, Oda Y, Tabata T, Sato T, Nagasu T, Rappsilber J, Mann M: Exponentially modified protein abundance index (emPAI) for estimation of absolute protein amount in proteomics by the number of sequenced peptides per protein. Mol Cell Proteomics 2005;4:1265-1272.
24 Bindea G, Galon J, Mlecnik B: CluePedia Cytoscape plugin: pathway insights using integrated experimental and in silico data. Bioinformatics 2013;29:661-663.
25 Trindade F, Ferreira R, Magalhaes B, Leite-Moreira A, Falcao-Pires I, Vitorino R: How to use and integrate bioinformatics tools to compare proteomic data from distinct conditions? A tutorial using the pathological similarities between Aortic Valve Stenosis and Coronary Artery Disease as a case-study. J Proteomics 2018;171:37-52.
26 Romero-Calvo I, Ocon B, Martinez-Moya P, Suarez MD, Zarzuelo A, Martinez-Augustin O, de Medina FS: Reversible Ponceau staining as a loading control alternative to actin in Western blots. Anal Biochem 2010;401:318-320.
27 Packer M: Epicardial Adipose Tissue May Mediate Deleterious Effects of Obesity and Inflammation on the Myocardium. J Am Coll Cardiol 2018;71:2360-2372.
28 Marchington JM, Mattacks CA, Pond CM: Adipose tissue in the mammalian heart and pericardium: structure, foetal development and biochemical properties. Comp Biochem Physiol B 1989;94:225-232.
29 Song DK, Hong YS, Lee H, Oh JY, Sung YA, Kim Y: Increased Epicardial Adipose Tissue Thickness in Type 2 Diabetes Mellitus and Obesity. Diabetes Metab J 2015;39:405-413.
30 Northcott JM, Yeganeh A, Taylor CG, Zahradka P, Wigle JT: Adipokines and the cardiovascular system: mechanisms mediating health and disease. Can J Physiol Pharmacol 2012;90:1029-1059.
31 Fuster JJ, Ouchi N, Gokce N, Walsh K: Obesity-Induced Changes in Adipose Tissue Microenvironment and Their Impact on Cardiovascular Disease. Circ Res 2016;118:1786-1807.
32 Conceicao GG, Miranda-Silva D, Alves E, Rodrigues P, Wust R, Sena C, Magalhaes J, Seica R, Leite-Moreira AF, Falcao-Pires I: Implications of mitochondrial dysfunction in heart failure with preserved ejection fraction. Eur J Heart Fail 2016;18:164-165.
33 Shin EJ, Schram K, Zheng XL, Sweeney G: Leptin attenuates hypoxia/reoxygenation-induced activation of the intrinsic pathway of apoptosis in rat H9c2 cells. J Cell Physiol 2009;221:490-497.
34 Rodriguez-Penas D, Feijoo-Bandin S, Garcia-Rua V, Mosquera-Leal A, Duran D, Varela A, Portoles M, Rosello-Lleti E, Rivera M, Dieguez C, Gualillo O, Gonzalez-Juanatey JR, Lago F: The Adipokine Chemerin Induces Apoptosis in Cardiomyocytes. Cell Physiol Biochem 2015;37:176-192.
35 Ballal K, Wilson CR, Harmancey R, Taegtmeyer H: Obesogenic high fat western diet induces oxidative stress and apoptosis in rat heart. Mol Cell Biochem 2010;344:221-230.

36 Chen D, Li X, Zhang L, Zhu M, Gao L: A high-fat diet impairs mitochondrial biogenesis, mitochondrial dynamics, and the respiratory chain complex in rat myocardial tissues. J Cell Biochem 2018;119:9602.
37 Serra D, Mera P, Malandrino MI, Mir JF, Herrero L: Mitochondrial fatty acid oxidation in obesity. Antioxid Redox Signal 2013;19:269-284.
38 Boden G: Obesity and free fatty acids. Endocrinol Metab Clin North Am 2008;37:635-646, viii-ix.
39 Rutkowski JM, Stern JH, Scherer PE: The cell biology of fat expansion. J Cell Biol 2015;208:501-512.
40 Cedikova M, Kripnerova M, Dvorakova J, Pitule P, Grundmanova M, Babuska V, Mullerova D, Kuncova J: Mitochondria in White, Brown, and Beige Adipocytes. Stem Cells Int 2016;2016:6067349.
41 Calderon-Dominguez M, Mir JF, Fucho R, Weber M, Serra D, Herrero L: Fatty acid metabolism and the basis of brown adipose tissue function. Adipocyte 2016;5:98-118.
42 Aldiss P, Davies G, Woods R, Budge H, Sacks HS, Symonds ME: 'Browning' the cardiac and peri-vascular adipose tissues to modulate cardiovascular risk. Int J Cardiol 2017;228:265-274.
43 Mazurek T, Zhang L, Zalewski A, Mannion JD, Diehl JT, Arafat H, Sarov-Blat L, O'Brien S, Keiper EA, Johnson AG, Martin J, Goldstein BJ, Shi Y: Human epicardial adipose tissue is a source of inflammatory mediators. Circulation 2003;108:2460-2466.
44 Bertero E, Maack C: Metabolic remodelling in heart failure. Nat Rev Cardiol 2018;15:457-470.